

FIG. 2. Photoluminescence spectra comparison of 1170 nm In<sub>0.35</sub>Ga<sub>0.65</sub>As QW and 1210 nm In<sub>0.4</sub>Ga<sub>0.6</sub>As QW active region.

regions of 100 Å GaAs on each side. The strain compensation of the active region is provided by the 75 Å GaAs<sub>0.85</sub>P<sub>0.15</sub> tensile barriers, which are grown before and after the GaAs barrier regions. The optical confinement factor for the InGaAs QW is calculated as approximately 1.7%. The growth of the active region and the optical confinement regions utilize an [AsH<sub>3</sub>]/III ratio in excess of 100, at a reactor temperature of approximately 530 °C. The *n*- and *p*-cladding layers are based on an Al<sub>0.74</sub>Ga<sub>0.26</sub>As material system, grown at 775 °C and 640 °C, respectively. Both cladding layers are designed with a doping level of approximately 1 × 10<sup>18</sup> cm<sup>-3</sup>. The tensile buffer layer consists of a 30 Å GaAs<sub>0.67</sub>P<sub>0.33</sub>, which we found to be crucial for the growth of the highly strained InGaAs(N) QW material system on top of a high Al-content lower cladding layer.<sup>6,7</sup>

The room-temperature photoluminescence of the 60 Å In<sub>0.4</sub>Ga<sub>0.6</sub>As QW active material is presented in Fig. 2, along with that of an 80 Å In<sub>0.35</sub>Ga<sub>0.65</sub>As QW for comparison. The peak emission wavelength of the In<sub>0.4</sub>Ga<sub>0.6</sub>As QW is measured at approximately 1210–1215 nm, which is 50–60 nm longer than that of the In<sub>0.35</sub>Ga<sub>0.65</sub>As QW. The reduction in the optical luminescence intensity of the In<sub>0.4</sub>Ga<sub>0.6</sub>As QW ( $\Delta a/a = 2.78\%$ ), in comparison to that of In<sub>0.35</sub>Ga<sub>0.65</sub>As QW ( $\Delta a/a = 2.45\%$ ), is presumably a result of a slight degradation in the crystal quality due to the higher strain of the 1210 nm InGaAs QW.

The lasing characteristics are measured under a pulsed condition with a pulse width of 5 μs and duty cycle of 1%. The measurements are performed on as-cleaved broad area laser devices, with an oxide-defined stripe width of 100 μm. The metal contacts are realized with 250 Å Ti/500 Å Pt/1500 Å Au and 200 Å Ge/1000 Å GeAu/500 Å Ni/3000 Å Au for *p* and *n* contacts, respectively. The contact annealing of the devices is accomplished under forming gas (10% H<sub>2</sub> + 90% N<sub>2</sub>) at a temperature of 370 °C for duration of 30 s.

The room-temperature ( $T = 20\text{ °C}$ ) lasing spectrum for the 60 Å In<sub>0.4</sub>Ga<sub>0.6</sub>As QW devices with a cavity length of 1000 μm is measured as long as 1233 nm, as shown in Fig. 3. The lasing emission wavelengths range from 1216 nm to 1233 nm, with little variation in threshold current densities. As shown in Fig. 3, the threshold current density of these In<sub>0.4</sub>Ga<sub>0.6</sub>As QW laser devices is found to be 90–92 A/cm<sup>2</sup> for measurements at a heat-sink temperature of 20 °C. The

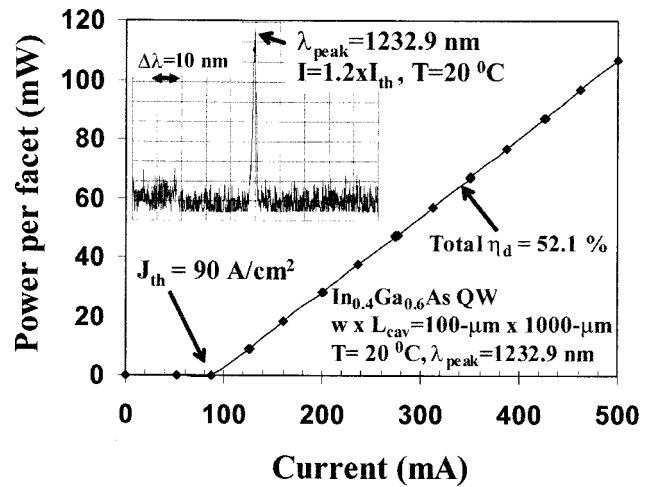


FIG. 3. The relation of output power per facet (*P*) and the total injected current (*I*) for In<sub>0.4</sub>Ga<sub>0.6</sub>As QW lasers with a cavity length of 1000 μm at a temperature of 20 °C. The inset shows the lasing spectrum at 20 °C.

total external differential quantum efficiency ( $\eta_d$ ) of the devices is measured as approximately 52.1%.

The temperature characteristics of the threshold current densities ( $T_0$  values, with  $1/T_0 = (1/J_{th}) \cdot dJ_{th}/dT$ ) and the external differential quantum efficiencies ( $T_1$  values, with  $1/T_1 = (-1/\eta_d) \cdot d\eta_d/dT$ ) of the 1233 nm In<sub>0.4</sub>Ga<sub>0.6</sub>As QW lasers are shown in Fig. 4. The temperature characterization is conducted from a temperature of 10 °C up to a temperature of 100 °C, with temperature steps of 5 °C. In the temperature range of 10 °C to 50 °C, the slope efficiency ( $\eta_d$ ) hardly decreases with temperature, resulting in a  $T_1$  value of approximately 1250 K based on our best fit. For the temperature range of 50 °C to 100 °C, we observe a significant drop of the  $T_1$  value from 1250 K to approximately 480 K. It is important to note that  $T_1$  values of 1250 K and 480 K are significantly larger than those of 1300 nm InGaAsN QW lasers. For 1300 nm InGaAsN QW lasers with the same separate confinement heterostructure as the InGaAs active lasers and cavity length of 1000 μm, we previously reported  $T_1$  value of 255 K for measurements in the temperature range of 20 °C to 60 °C. The  $T_0$  values are measured as 140 K and 105 K for measurements in the temperature ranges of 10–50 °C and 50–100 °C, respectively. The lowering of  $T_0$  and  $T_1$  values at elevated temperatures are presumably driven by the thermionic carrier leakage processes. Neverthe-

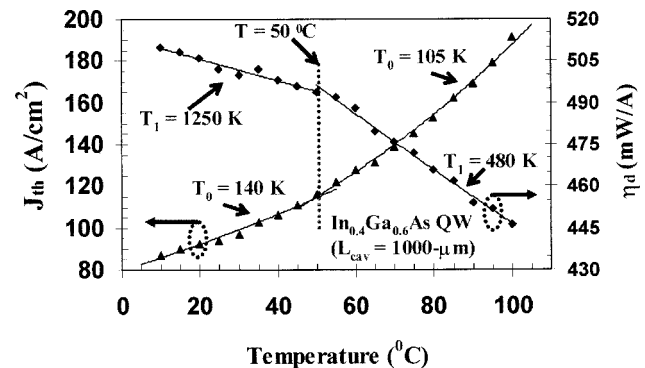


FIG. 4. Threshold current density ( $J_{th}$ ) and external differential quantum efficiency ( $\eta_d$ ) of 1233 nm In<sub>0.4</sub>Ga<sub>0.6</sub>As QW lasers ( $L_{cav} = 1000\text{ }\mu\text{m}$ ) as a function of temperature in the range of 10 °C to 100 °C.

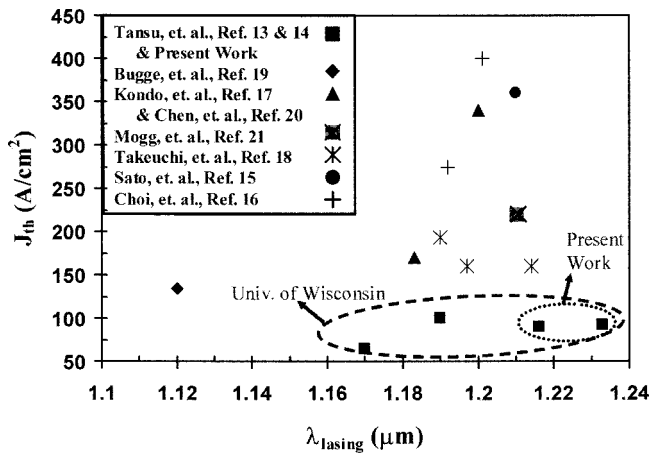


FIG. 5. Comparison of threshold current densities of InGaAs QW lasers in the 1100–1250 nm wavelength regime.

less, very-low threshold-current-densities of only 160 A/cm<sup>2</sup> and 190 A/cm<sup>2</sup> are achieved for In<sub>0.4</sub>Ga<sub>0.6</sub>As QW lasers ( $L_{\text{cav}}=1000 \mu\text{m}$ ) at temperatures of 85 °C and 100 °C, respectively.

Comparison of the lasing characteristics of the 1215–1233 nm InGaAs QW lasers with reported results in literature<sup>13–21</sup> is shown in Fig. 5. As the emission wavelength of the InGaAs QW lasers is extended, typically, their threshold current densities increase rapidly. Previously, very low reported threshold current densities for InGaAs QW lasers on GaAs beyond emission wavelength of 1210 nm were realized by Takeuchi and co-workers<sup>18</sup> with room-temperature threshold current densities of 160 A/cm<sup>2</sup> for devices with cavity length of 1000  $\mu\text{m}$ . In our present work, we recorded threshold current densities of only 90–92 A/cm<sup>2</sup> for strain-compensated InGaAs QW lasers up to emission wavelength of 1233 nm. It is also important to note that we observe only a very slight dependence of the threshold current densities on emission wavelengths from 1170 nm to 1233 nm, which may be a result of the utilization of the GaAsP tensile-strained barriers.

In summary, high-performance InGaAs QW lasers have been realized with lasing performance up to an emission wavelength of 1233 nm. The realization of diode lasers with a room-temperature emission wavelength of 1233 nm, represents the longest emission wavelength realized with only an InGaAs QW active region on a GaAs substrate. The thresh-

old current densities of only 90 A/cm<sup>2</sup> and 190 A/cm<sup>2</sup> are measured for laser devices with a cavity length of 1000  $\mu\text{m}$  at temperatures of 20 °C and 100 °C, respectively. These reported threshold current densities represent among the lowest values for InGaAs QW diode lasers on GaAs in the wavelength regime beyond 1200 nm. No evidence of a significant increase in the threshold current of the InGaAs QW lasers, with increasing wavelength beyond 1200 nm, indicates the potential for achieving high-performance diode lasers on GaAs substrates with emission wavelength even beyond 1233 nm utilizing only an InGaAs QW active material.

- <sup>1</sup>G. L. Belenky, C. L. Reynolds, Jr., D. V. Donetsky, G. E. Shtengel, M. S. Hybertsen, M. A. Alam, G. A. Baraff, R. K. Smith, R. F. Kazarinov, J. Winn, and L. E. Smith, *IEEE J. Quantum Electron.* **35**, 1515 (1999).
- <sup>2</sup>M. Kondow, T. Kitatani, S. Nakatsuka, M. C. Larson, K. Nakahara, Y. Yazawa, M. Okai, and K. Uomi, *IEEE J. Sel. Top. Quantum Electron.* **3**, 719 (1997).
- <sup>3</sup>J. S. Harris, Jr., *IEEE J. Sel. Top. Quantum Electron.* **6**, 1145 (2000).
- <sup>4</sup>S. Sato, *Jpn. J. Appl. Phys., Part 1* **39**, 3403 (2000).
- <sup>5</sup>D. A. Livshits, A. Y. Egorov, and H. Riechert, *Electron. Lett.* **36**, 1381 (2000).
- <sup>6</sup>N. Tansu and L. J. Mawst, *IEEE Photonics Technol. Lett.* **14**, 444 (2002).
- <sup>7</sup>N. Tansu, N. J. Kirsch, and L. J. Mawst, *Appl. Phys. Lett.* **81**, 2523 (2002).
- <sup>8</sup>J. Wei, F. Xia, C. Li, and S. R. Forrest, *IEEE Photonics Technol. Lett.* **14**, 597 (2002).
- <sup>9</sup>K. D. Choquette, J. F. Klem, A. J. Fischer, O. Blum, A. A. Allerman, I. J. Fritz, S. R. Kurtz, W. G. Breiland, R. Sieg, K. M. Geib, J. W. Scott, and R. L. Naone, *Electron. Lett.* **36**, 1388 (2000).
- <sup>10</sup>W. Ha, V. Gambin, M. Wistey, S. Bank, S. Kim, and J. S. Harris, Jr., *IEEE Photonics Technol. Lett.* **14**, 591 (2002).
- <sup>11</sup>C. S. Peng, T. Jouhti, P. Laukkanen, E.-M. Pavelescu, J. Konttinen, W. Li, and M. Pessa, *IEEE Photonics Technol. Lett.* **14**, 275 (2002).
- <sup>12</sup>N. Tansu, J. Y. Yeh, and L. J. Mawst (unpublished).
- <sup>13</sup>N. Tansu and L. J. Mawst, *IEEE Photonics Technol. Lett.* **13**, 179 (2001).
- <sup>14</sup>N. Tansu, Y. L. Chang, T. Takeuchi, D. P. Bour, S. W. Corzine, M. R. T. Tan, and L. J. Mawst, *IEEE J. Quantum Electron.* **38**, 640 (2002).
- <sup>15</sup>S. Sato and S. Satoh, *Jpn. J. Appl. Phys., Part 2* **38**, L990 (1999).
- <sup>16</sup>W. Choi, P. D. Dapkus, and J. Jewell, *IEEE Photonics Technol. Lett.* **11**, 1572 (1999).
- <sup>17</sup>T. Kondo, D. Schlenker, T. Miyamoto, Z. Chen, M. Kawaguchi, E. Gouardes, F. Koyama, and K. Iga, *Jpn. J. Appl. Phys., Part 1* **40**, 467 (2000).
- <sup>18</sup>T. Takeuchi, Y.-L. Chang, A. Tandon, D. Bour, S. Corzine, R. Twist, M. Tan, and H.-C. Luan, *Appl. Phys. Lett.* **80**, 2445 (2002).
- <sup>19</sup>F. Bugge, G. Erbert, J. Fricke, S. Gramlich, R. Staske, H. Wenzel, U. Zeimer, and M. Weyers, *Appl. Phys. Lett.* **79**, 1965 (2001).
- <sup>20</sup>Z. B. Chen, D. Schlenker, F. Koyama, T. Miyamoto, A. Matsutani, and K. Iga, in *Proceedings of the APCC/OECC'99*, Beijing, China, 1999, Vol. 2, p. 1311.
- <sup>21</sup>S. Mogg, N. Chitica, R. Schatz, and M. Hammar, *Appl. Phys. Lett.* **81**, 2334 (2002).